Comparison of condensation heat transfer on hydrophobic and nano-porous surface

Taeseok Kim[a], Sung Joong Kim[a,b*], Jaemin Lee[c], Wonjoon Choi[c]
[a]*Department of Nuclear Engineering, Hanyang University, 222 Wangsimni-ro, Seongdong-gu, Seoul 04763 Republic of Korea*
[b] *Institute of Nano Science & Technology, Hanyang University, 222 Wangsimni-ro, Seongdong-gu, Seoul 04763 Republic of Korea*
[c] *School of Mechanical Engineering, Korea University, 145 Anam-ro, Seongbuk-gu, Seoul 02841, Republic of Korea*
[*]*Corresponding author: sungjkim@hanyang.ac.kr*

1. Introduction

Condensation is widely used in many engineering fields, such as water desalination [1], water harvesting [2], thermal management system [3], and safety system in nuclear industry [4]. Especially, the condensation heat transfer mitigates pressurization following a severe accident of the nuclear power plants [5]. Passive containment cooling system (PCCS) condensates a large amount of steam to depressurization in containment and removes decay heat using condensation heat transfer. Therefore, the condensation heat transfer performance is related efficiency of the safety feature in the nuclear power plants.

It is well known that surface characteristics such as wettability, topography are highly correlated to the condensation heat transfer. For example, Parin [6] investigated the roughness effect to the condensation heat transfer, and the highly rough surface has 8 times higher condensation heat transfer coefficient than an untreated surface. Izumi [7] used vertical groove surface and enhanced the condensation heat transfer about 25% than other surfaces. Preston [8] promotes dropwise condensation using chemical vapor deposition (CVD) graphene, so it increases the condensation heat transfer coefficient. There are many studies about the surface effect even if it doesn't control surface topography. Rykaczewski et al. [9] used oleophobic surfaces to the condensation experiment and enhanced the condensation heat transfer coefficient. Chatterjee [10] perform the condensation heat transfer experiment using hydrophilic and hydrophobic patterned surfaces.

Accordingly, the many researchers have targeted the effects of single surface parameter to the condensation heat transfer. Few studies, however, have examined the combined effects of two or more variables of the surface parameter. In this study, we focused on the surface wettability and porous media effects on the condensation heat transfer.

2. Surface modification

2.1. Fabrication of PEI/MWCNT layer

LbL technique is a coating method to fabricate micro/nano structured film on surfaces of various substrates [11]. LbL is based on electrostatic forces between materials which are charged with different polarity. The charged materials can form layers that are adhesive and uniform along the substrate surface because of electrostatic forces. Compare to other coating methods, the LbL deposition can be used on large areas without specific equipment. Because of this usefulness, the LbL assembly technique has been used for surface thin film formation [12,13].

Multi-walled CNT (MWCNT) is known as excellent thermal property and chemical-mechanical stability, so it has raised much interest during the recent years [14]. The enhancement of condensation heat transfer using the MWCNT was reported by many researcher [15,16]. If it was applied carboxylic-functionalized methods, the MWCNT can be manufactured using LbL deposition. The MWCNTs were functionalized with carboxylic groups (-COOH), which made the negatively charged surface. As for the positively charged surface, polyethyleneimine (PEI) was used to fabricate the LbL assembly with the MWCNT. The fabrication process of the LbL assembled PEI/ MWCNT is presented in Figure 1. First, the substrate was immersed in the PEI 10 minutes, and washed particles are not deposited. In sequence, deep in the MWCNT solution in 10 minutes, it deposited one bi-layer of LbL-PEI/MWCNTs. In this study, a substrate of the LbL coating was deposited with 10 bilayers. This surface is called "CNT" in this paper.

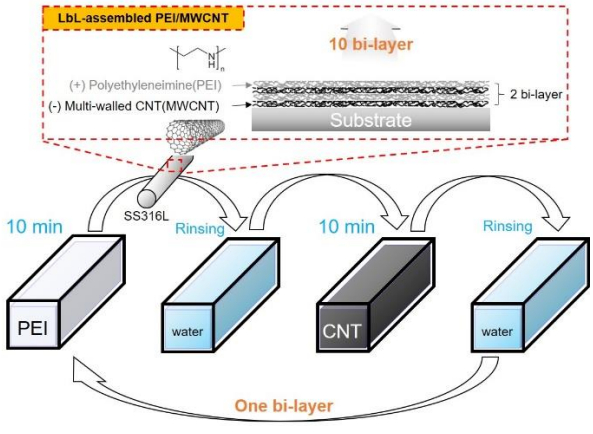

Fig. 1. Scheme for fabrication of LbL-assembled PEI/MWCNT coatings on the substrates

2.2. Deposition of OTS layer

Self-assembled monolayer (SAM) is organic assemblies formed by adsorption of molecular constituents from

solution on the solid surface [17]. SAM technique provides chemical functionality to the surface with the convenient and simple system. The surface modification using SAM also fabricated by the substrates immersed in the coating solution material such as alkylsilane [18]. The surface deposited by SAM has different functionality and affinity by the solution material and substrate. Especially, head group and terminal group of solution material are decided the functionality and affinity of the surface.

In this study, octadecyltrichlorosilane (OTS) which has a methyl group (-CH3) as the terminal group was used for the solution material. The methyl group on SAM makes the surface to hydrophobic functionality, so the hydrophobic functionalization of the surface was conducted by the OTS. The SAM coating was performed by immersing the substrates into an anhydrous toluene solution of 1 mM OTS. The effect of immersion time on SAM formation was saturated after 2 hours in the previous study [19], so this study followed the immersion time as 2 hours. And then, annealing was performed by 120 ºC to crosslink silicon molecular of the OTS each other. The SAM deposition does not change surface morphology because the OTS molecular size is almost 2~3 nm [20]. Unchanged surface morphology retains the nano-porous structure of the LbL assembled PEI/MWCNT surface. Figure 2 shows the schematic of the SAM deposition of the OTS. The detailed information about the OTS coating on the stainless steel is available in reference [19].

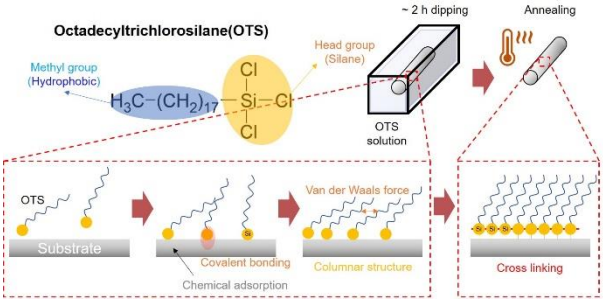

Fig. 2. Scheme for fabrication of OTS monolayer coatings on the substrates

2.3. Contact angle measurement

The contact angle is a representative quantified factor of the surface wettability. It was measured using the Kruss EasyDrop which is the contact angle measurement equipment. Figure 3 shows the static contact angles of the bare, CNT, OTS and CNT+OTS. The contact angle of the untreated bare substrate was about 74º. The CNT was shown a lower contact angle about 20º, it means that the surface turns to the hydrophilic surface. This is because the nano-porous structure of the CNT surface causes capillary wicking to imbibe the water. On the other hand, the OTS and CNT+OTS surfaces have higher contact angle than the bare surface. The functionality of the methyl group of OTS makes the surface hydrophobic. The CNT+OTS surface also was deposited CNT on the surface, but the OTS was piled up on the nano-porous structure of the CNT. Thus, the CNT+OTS also had hydrophobicity on the surface as shown in Figure 3.

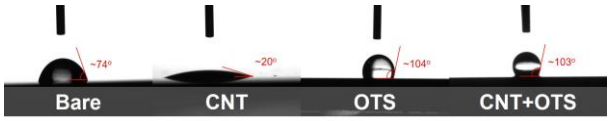

Fig. 3. A contact angle of each surface

2.4. Surface morphologies of CNT coating

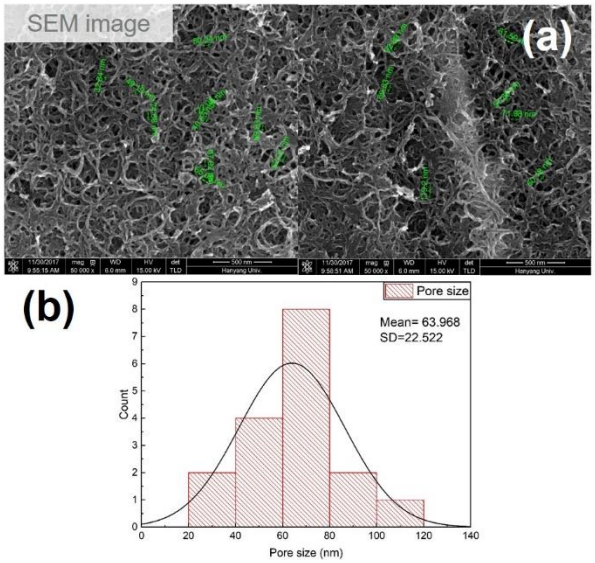

Fig. 4. (a) SEM images of CNT layers, (b) the pore size distribution of the CNT surface

The CNT surface was studied by many researchers due to the enhancement of the condensation heat transfer [15,16]. This is because that the LbL assembled PEI/MWCNT coating makes nano-porous structures which is randomly generated MWCNTs networks on the substrates. To investigate the condensation heat transfer performance of the nano-porous structure, many surface factors related porous media were used in recent researches [21]. The surface characteristic factor of the porous structure has been analyzed such as pore diameter, porosity and porous layer thickness. In this study, to characterize the nano-porous structure of CNT surface, visualization of the surface was conducted by SEM image. Figure 4 (a) shows a 50,000x magnified SEM images on the CNT coating surfaces. The CNT surface shows that many MWCNT fibers construct the nano-porous structures on the surface. The quantification of surface parameters related to porous media is difficult due to the nano scale of factors. However, the pore size can be quantified roughly using distance measurement in SEM images. Figure 4 shows a 50,000x magnified Scanning electron microscopy (SEM) images of the CNT surface and the measurement of the pore size. Because of intrinsic randomness of LbL deposition, the pore size has a large band from 30 to 120. Figure 4 (b) shows

histogram of the pore size and result using a statistic tool of Origin Pro. The average size of the pore size was measured by 63.968 nm and standard deviation was 22.522 as shown in Figure 4 (b).

3. Condensation heat transfer experiment

3.1. Experimental set up

The condensation heat transfer experiment system is illustrated in Figure 5 by isometric drawing. The test section was vertical tube made of stainless steel 316 and the length, diameter and thickness are 300 mm, 19.05 mm and 1.24 mm, respectively. The inside of test section, the coolant flowed upstream direction and the saturated steam is condensed on the outside wall of the test section. The saturated steam supplied from 18 kW steam generator to steam chamber through steam/water separator. If the steam is condensed, the condensed water flowed to drain tank. The coolant used DI water at atmospheric pressure, and the coolant temperature and flow rate were controlled by proportional-integral-derivative (PID) control and coolant pump, respectively. Visualization of condensation test was conducted using a high-speed video system (Phantom V7.3 high speed camera). In this paper, the coolant mass flux and the steam pressure were kept to 415 kg/m2s and 55 kPa gauge, respectively.

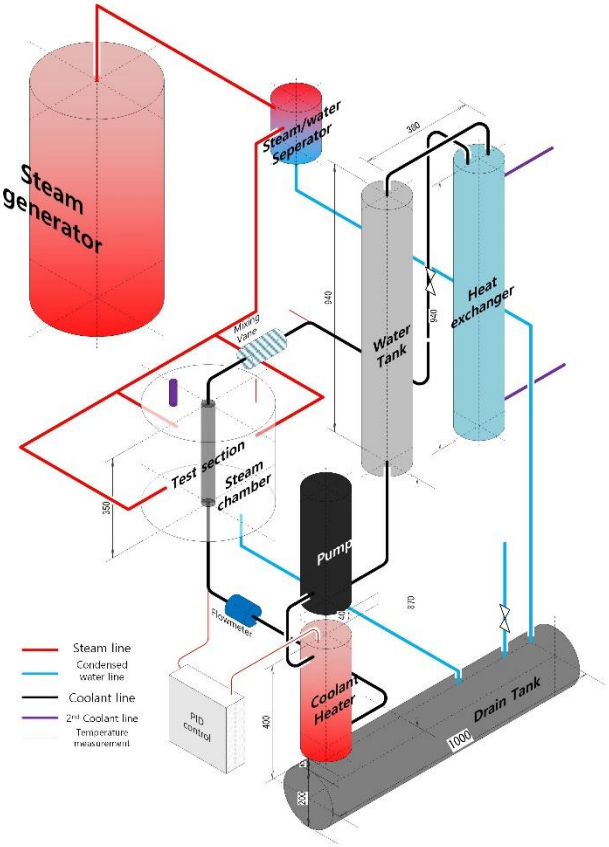

Fig. 5. Schematics of condensation heat transfer experiment system

3.2. Experiment result

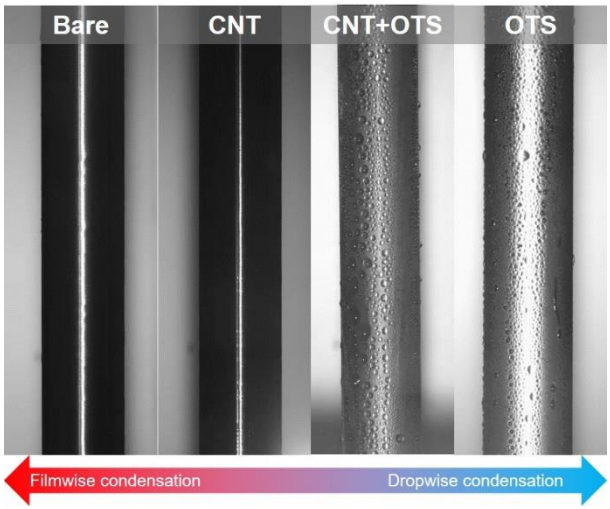

Fig. 6. Visualization of the condensation on each surface

First, we took high speed images to determine a mode of condensation "filmwise condensation" or "dropwise condensation". The dropwise condensation is more efficient to transfer heat because of thermal resistance of liquid film in the filmwise condensation [22]. In this study, each surface had a different condensation mode. The bare and CNT surfaces showed the filmwise condensation, the CNT+OTS and the OTS surface showed dropwise condensation as shown in Figure 6. It is well known that the surface wettability is highly related to the condensation mode. In the bare and CNT surfaces has relatively hydrophilic than the others, so it had filmwise condensation in the experiment. On the other hand, the CNT+OTS and OTS surfaces are hydrophobic surface, so these surfaces had dropwise condensation. This condensation mode is directly connected to the condensation heat transfer performance.

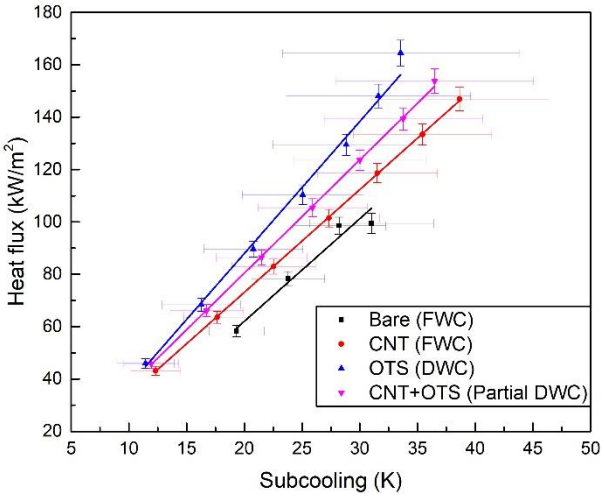

Fig. 7. Heat flux related condensation heat transfer of each surface

Figure 7 shows the condensation heat flux versus average wall subcooling. The bare has lowest condensation heat flux, followed by the CNT surface. On the other hand, the OTS surface has a highest condensation heat flux, followed by the CNT+OTS surface. Most of them are followed the condensation mode, which is mentioned in the Figure 6. However, the CNT surface had much condensation heat transfer performance than the bare surface even though they have a same condensation mode of filmwise condensation. It is because the porous media of the CNT layers enhanced heat transfer from the tube to the condensed water. The porous layer has more heat transfer area than the plane surface, so it causes high heat transfer performance. On the other hand, the difference between CNT+OTS and OTS is caused by coating thickness. The CNT layer thickness is about 250 nm, it is thicker than the OTS layer which has just about 10 nm thickness. This difference of thickness causes different thermal resistance, so the condensation heat transfer performance is different between CNT+OTS and OTS.

4. Conclusion

In this work, the effect of the CNT and OTS layers and the combined effect of the CNT and OTS coating to the condensation heat transfer have been studied. The OTS deposition makes the surface hydrophobic, and the CNT coating piles up the porous media on the surface. These surfaces characteristic causes the condensation mode of each surface; bare and CNT are filmwise, CNT+OTS and OTS are dropwise condensation. Finally, it is related to the condensation heat transfer coefficient; OTS > CNT+OTS > CNT > bare. This result paves a new path of employing hydrophobic and nano-porous coatings to enhance the condensation heat transfer. Future work should focus on the surface parameter related to the condensation heat transfer

REFERENCES

[1] S. Parekh et al., “Solar desalination with a humidification-dehumidification technique — a comprehensive technical review,” Desalination 160(2), pp. 167-186 (2004).
[2] V. Wahlgren, “Atmospheric water vapour processor designs for potable water production: a review,” Water Res. 35(1), pp. 1-22 (2001).
[3] C. Nadjahi, H. Louahlia, and S. Lemasson, “A review of thermal management and innovative cooling strategies for data center,” Sustain. Comput. Informatics Syst. 19, pp. 14-28 (2018).
[4] S. W. Lee et al., “The concept of the innovative power reactor,” Nucl. Eng. Technol. 49(7), pp. 1431-1441 (2017).
[5] I. K. Huhtiniemi and M. L. Corradini, “Condensation in the presence of noncondensable gases,” Nucl. Eng. Des. 141(3), pp. 429-446 (1993).
[6] R. Parin et al., “Nano-structured aluminum surfaces for dropwise condensation,” Surf. Coatings Technol. 348, pp. 1-12, (2018).
[7] M. Izumi et al., “Heat transfer enhancement of dropwise condensation on a vertical surface with round shaped grooves,” Exp. Therm. Fluid Sci. 28(2–3), pp. 243-248 (2004).
[8] D. J. Preston et al., “Scalable graphene coatings for enhanced condensation heat transfer,” Nano Lett. 15(5), pp. 2902-2909 (2015).
[9] K. Rykaczewski et al., “Dropwise condensation of low surface tension fluids on omniphobic surfaces,” Sci. Rep. 4, pp. 1-8 (2014).
[10] A. Chatterjee et al., “Enhancement of condensation heat transfer with patterned surfaces,” Int. J. Heat Mass Transf. 71, pp. 675-681 (2014).
[11] J. J. Richardson, M. Bjornmalm, and F. Caruso, “Technology-driven layer-by-layer assembly of nanofilms,” Science. 348 (6233), pp. aaa2491-aaa2491 (2015).
[12] S. W. Lee et al., “Layer-by-Layer Assembly of All Carbon Nanotube Ultrathin Films for Electrochemical Applications,” J. Am. Chem. Soc. 131(2), pp. 671-679 (2009).
[13] M. Olek et al., “Layer-by-layer assembled composites from multiwall carbon nanotubes with different morphologies,” Nano Lett. 4(10), pp. 1889-1895 (2004).
[14] V. Datsyuk et al., “Chemical oxidation of multiwalled carbon nanotubes,” Carbon. 46(6), pp. 833-840 (2008).
[15] G. Udaya Kumar et al., “Investigating the combined effect of square microgrooves and CNT coating on condensation heat transfer,” Appl. Surf. Sci. 469, pp. 50-60 (2019).
[16] S. Lee et al., “Heat transfer measurement during dropwise condensation using micro/nano-scale porous surface,” Int. J. Heat Mass Transf. 65, pp. 619-626 (2013).
[17] Y.S. Chi, S. Kang and I.S. Choi, “Surface Engineering Based on Self-Assembled Monolayers,” Polymer Sci. Technol. 17(2), pp. 172-181 (2006).
[18] G. Mani et al., “Surface modification of cobalt-chromium-tungsten-nickel alloy using octadecyltrichlorosilanes,” Appl. Surf. Sci. 255(11), pp. 5961-5970 (2009).
[19] Z. Zhu et al., “Construction of octadecyltrichlorosilane self-assembled monolayer on stainless steel 316L surface,” Colloids Surfaces A Physicochem. Eng. Asp. 457(1), pp. 408-413 (2014).
[20] R. Wen et al., “Hydrophobic copper nanowires for enhancing condensation heat transfer,” Nano Energy 33 January, pp. 177-183 (2017).
[21] E. Barsotti et al., “A review on capillary condensation in nanoporous media: Implications for hydrocarbon recovery from tight reservoirs,” Fuel 184, pp. 344-361 (2016).
[22] Carey, Van P. Liquid vapor phase change phenomena: an introduction to the thermophysics of vaporization and condensation processes in heat transfer equipment. CRC Press, (2018).